

The Peroxidase–NADH Biochemical Oscillator. 1. Examination of Oxygen Mass Transport, the Effect of Light, and the Role of Methylene Blue

Dean L. Olson[†] and Alexander Scheeline^{*‡}

Department of Chemistry, University of Illinois at Urbana–Champaign, 600 S. Mathews,
Urbana, Illinois 61801

Received: May 30, 1994; In Final Form: November 14, 1994[⊗]

The peroxidase–NADH oscillator examined here initially consists of four chemical components. The well-mixed aqueous solution includes native horseradish peroxidase, reduced β -nicotinamide adenine dinucleotide (NADH), methylene blue (MB^+), and dissolved oxygen combined in a semi-batch reactor under a set of standard conditions. In this system, the macroscopic appearance of the process of oxygen dissolution from the gas phase is dependent on k_m , the mass transport constant of oxygen out of solution. Additional details of oxygen mass transport are derived. The amplitude of oxygen oscillations is decreased by continuous illumination by the deuterium source of a diode array spectrophotometer. This attenuation effect of light is dependent on wavelengths ≤ 248 nm. Initial omission of MB^+ allows several damped oscillations of small amplitude. Subsequent addition of MB^+ to the oscillator results in oscillations of much larger amplitude. MB^+ is seen to either directly or indirectly enhance the conversion of peroxidase compound III to the native enzyme and then inhibit oxygen consumption, allowing the initiation of relatively large, prolonged oscillations. MB^+ is seen to function either as a system catalyst, or as a peroxidase inhibitor in the oxidation of NADH by oxygen.

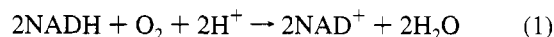
Introduction

Enzyme-based reactions have been implicated as the molecular basis of a wide range of cyclic biological functions including cellular operations,¹ biochemical switches,^{2–4} and circadian rhythms.⁵ The concentrations of chemical species in such systems can vary periodically as a function of time. Though a great deal of knowledge exists on the metabolic and regulatory properties of enzymes in biological systems, relatively few attempts have been made to expand this information into realistic models which exhibit nonlinear temporal behavior.⁶

The in vitro aerobic oxidation of reduced β -nicotinamide adenine dinucleotide (NADH) catalyzed by the enzyme horseradish peroxidase (HRP) is the first single-enzyme system directly observed to display cyclic behavior. Under specific conditions, the concentrations of several chemical species exhibit oscillations as a function of time. First reported in 1965,⁷ the peroxidase–NADH system is one of the few biochemical examples among known in vitro oscillators, the majority of which are based on inorganic species.^{8,9} Peroxidase is a biologically common heme glycoprotein found in both plants and animals,¹⁰ and NADH is ubiquitous in biological systems as an electron carrier. Consequently, this system can serve as an in vitro analogue for the development of methods and principles to directly observe and study the nonlinear dynamics of cyclic, biochemical reactions.

The peroxidase–NADH oscillator traditionally has been studied as an open system of five chemical species combined in a semi-batch reactor. The well-mixed, aqueous solution initially consists of native horseradish peroxidase (Per^{3+}), methylene blue (MB^+), and 2,4-dichlorophenol (DCP), to which NADH and oxygen are added at constant rates. Specific conditions result in oscillations in the concentration of numerous species over the course of several hours. The peroxidase-

catalyzed oxidation of NADH



is a dominant reaction. The modifiers MB^+ and DCP were introduced in 1973¹¹ to eliminate oscillatory damping and were initially described as having the ability to (respectively) activate and sustain the oscillations in an unknown way. Recently, a hypothesis was suggested for the chemical role of MB^+ which involved the catalytic oxidation of NADH by MB^+ .^{12,13}

A significant number of papers on this oscillator have appeared which report a variety of nonlinear behaviors, including sustained oscillations,¹¹ bistability,¹⁴ chaos,^{15–17} and a period-doubling approach to chaos.¹⁸ Studies of various inorganic oscillators have revealed that complex, nonlinear rate laws (higher or nonintegral order) are commonly involved in oscillatory chemical behavior.⁹ Autocatalysis or self-inhibition of a species is often found, and a delayed feedback mechanism is usually required to give rise to oscillations. Oscillatory reactions must be maintained far from equilibrium; this is accomplished here by continuous addition of NADH and oxygen. Many models which include these features have been proposed for the peroxidase–NADH oscillator.^{6,19–22}

A standardized model, termed the Urbanalator, was recently proposed to describe the simple oscillatory behavior.²³ This comprehensive, experimentally based chemical model includes all initial chemical species and several intermediates. An oscillation is caused by the decrease of native enzyme during the oxygen increase, where the oxidized form of the enzyme is held stable. The transformation of enzyme from the oxidized back to the native state occurs near the onset of oxygen decrease and is triggered by depletion of the native enzyme and controlled via several intermediates, particularly superoxide (O_2^-). Results reported here were obtained before conception of the Urbanalator and contributed significantly to its development.

Other previous research²⁴ focused on establishing a well-defined, controlled, and characterized experimental system to

[†] olson@c.scs.uiuc.edu.

[‡] scheeline@c.scs.uiuc.edu.

[⊗] Abstract published in *Advance ACS Abstracts*, January 1, 1995.

TABLE 1: Standard Conditions for the Peroxidase–NADH Oscillator

controlled variable	value
pH	5.10
buffer	0.100 M sodium acetate
horseradish peroxidase activity	100 pyrogallol units/mL (~7.9 μM)
oxygen mass-transport constant, k_m	0.123–0.208 min^{-1}
stirring rate	1300 rpm
resultant % O_2	1.50%
O_2 flow rate (2.10% O_2)	135.7 mL min^{-1}
N_2 flow rate	54.3 mL min^{-1}
solution volume	5.00 mL
solution surface area ^a	2.9 cm^2
temperature	25.00 $^\circ\text{C}$
reservoir [NADH] and buffer	6.37 mM (pH 7.00, 0.010 M NaAc)
NADH delivery rate	
initial	0.59 mM h^{-1} (465 $\mu\text{L h}^{-1}$, 35 lb in.^{-2})
maintenance ^b	0.39 mM h^{-1} (309 $\mu\text{L h}^{-1}$, 23 lb in.^{-2})
[methylene blue]	0.20 μM
illumination	total darkness, or continuous deuterium source for absorbance data
[2,4-dichlorophenol]	zero

^a This value is more accurate than the one reported previously.²⁴

^b The NADH delivery rate was changed from the initial to maintenance value at the second minimum observed in dissolved oxygen.

investigate the oscillator. The enhanced experimental approach, now in routine use by this group, includes thorough knowledge and careful control of 15 variables required to obtain meaningful results. Consistently defined and systematically controlled experimental parameters are essential to obtain reproducible data. Dissolved oxygen and multiwavelength UV–vis absorbance are monitored simultaneously over time. This multidimensional approach to data acquisition provides an improved experimental basis for more realistic analysis and modeling.

Under at least one set of conditions, the oscillatory system was reduced from five initial chemical components to just four, omitting DCP, which presumably simplifies the chemistry of the system. However, it is uncertain whether DCP omission increases or decreases the likelihood that non-DCP oscillations are actually biomimetic. Peroxidase is a phenol-dehydrogenating enzyme found in plants and is involved in the initial stages of lignin formation.²⁵ Polymerization of phenol monomers (in particular 4-hydroxylated cinnamyl alcohols) is initiated by the peroxidase-dependent formation of phenoxy radicals.²⁶ Though DCP is a nonbiological phenol, DCP and certain other biologically related phenols stimulate NADH oxidation by HRP.²⁷ If the oscillatory system studied here is a representation of that which occurs in real biological systems, it could reveal insights into how enzymatically controlled cyclic systems operate in nature. The standard conditions used for all of the following experiments appear in Table 1 and do not include DCP. MB^+ is necessary for prolonged oscillations under these conditions, but DCP is not.²⁴

Several papers have appeared^{28–31} which modify the chemistry of the oscillatory system described in Table 1. An additional enzyme, glucose-6-phosphate dehydrogenase, is added which recycles NAD^+ to NADH so that NADH does not need to be added continuously. This allows the use of a continuous-flow, stirred tank reactor (CSTR), where reactants are continuously added and withdrawn. The CSTR, widely used in the study of other oscillators, can provide long-term maintenance of a reaction far from equilibrium. For the peroxidase–NADH system, this CSTR approach also requires addition of a unique

enzyme substrate, glucose-6-phosphate, and the resultant formation of its reaction product, 6-phosphogluconolactone.²⁸ This adds three new chemical species to the system, yet only an unsubstantiated claim is made that the chemistry of the original oscillator is unaffected,²⁸ and this claim has been cited in additional papers by the same group^{29,30} and by another group.³¹ Systematic control of the present semi-batch system allows oscillations to be maintained for over 5 h, which makes a CSTR, its chemical additions, and its possible complications, unnecessary in these studies.

Experimental Section

The experimental system employed here was previously characterized and described in detail.²⁴ Unless noted otherwise, the standard conditions listed in Table 1, as previously discussed,²⁴ were used in all oscillatory experiments. The system consists of an aqueous, buffered solution of HRP, and methylene blue to which NADH is added at a constant, pulseless rate through a capillary from a pressurized reservoir. A mixture of oxygen and nitrogen is blown rapidly down onto the well-stirred solution. Water evaporation is offset by the influx of NADH solution. Dissolved oxygen is monitored using a Clark-type probe (Microelectrodes, Inc., Londonderry, NH). The electrode allows O_2 to pass through a semipermeable PTFE membrane where it is reduced at a platinum cathode. The resultant current is converted to voltage and then to a digital signal.²⁴ Oxygen data were taken at intervals of 10 s. The oscillatory mixture is contained in a quartz cuvette. A thermostating jacket for the cuvette rests in the spectrophotometer.

Note that in this paper, the error associated with a value derived from a replicate determination will be expressed as \pm percent RSD, the relative standard deviation in percent.

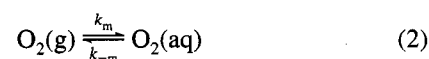
Reagents. Horseradish peroxidase was obtained as the salt-free lyophilized powder (E.C. 1.11.1.7; 90% isoenzyme C; Cat. No. 814393, MW = 42 100 g/mol; Boehringer Mannheim, Indianapolis, IN). Each HRP shipment was assayed before use; the activity is about 300 Sigma units/mg.²⁴ Methylene blue (MB^+) was obtained from Sigma as the chloride salt (Cat. No. MB-1).

All other chemicals used here are described elsewhere.²⁴ Throughout this paper, native HRP enzyme will be designated Per^{3+} , and compounds II, I, and III will be designated Per^{4+} , Per^{5+} , and Per^{6+} , respectively.

Illumination. A Hewlett-Packard ultraviolet–visible 8452A diode array spectrophotometer and HP 89531A software were used for all absorption measurements. Kinetics data were collected at intervals of 10 s, over an integration period of 10 s for each data point.

Results and Discussion

Oxygen Mass Transport. The process of oxygen mass transport is related to the experimental configuration (which includes a gas/liquid interface) used here and in all reported studies of the peroxidase–NADH oscillator since its discovery in 1965.⁷ Oxygen dissolution can be described by



where the rate law is

$$d[\text{O}_2]_{\text{aq}}/dt = k_m[\text{O}_2]_{\text{g}} - k_{-m}[\text{O}_2]_{\text{aq}} \quad (3)$$

and $[\text{O}_2]_{\text{g}}$ and $[\text{O}_2]_{\text{aq}}$ are the bulk concentrations of oxygen in the gas and aqueous phases, and k_m and k_{-m} are the apparent mass transport rate constants into and out of solution, respec-

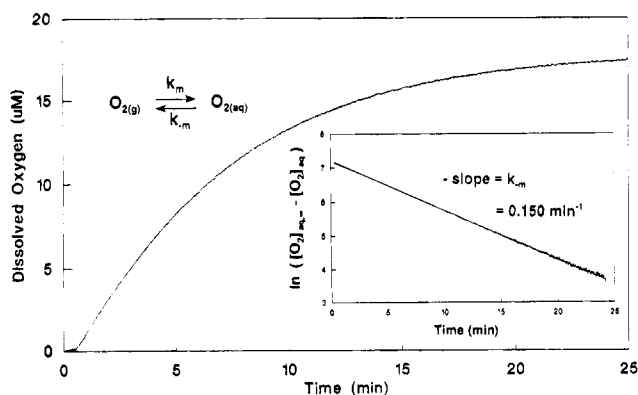


Figure 1. Exponential growth of dissolved oxygen used to compute k_m . With just Per^{3+} , MB^+ , and deoxygenated buffer in the cuvette at $t = 0$, the gas stream is switched from pure nitrogen to 1.50% oxygen. Dissolved O_2 is monitored for 25 min and linearized to yield $k_m = 0.150 \text{ min}^{-1}$, as shown in the inset and described in the text.

tively, for the partitioning of oxygen across the gas/liquid interface. Initially, the dissolved oxygen concentration $[\text{O}_2]_{\text{aq}} = 0$, and $[\text{O}_2]_{\text{g}} = \text{constant} = 613 \mu\text{M}$ (1.50% O_2 , 25 °C). The solution is rapidly stirred and gas flow is relatively fast, so the equilibration process is not diffusion limited. In addition to oxygen diffusion across the interface, the overall measured rate of oxygen dissolution is a function of temperature, ionic strength, $[\text{O}_2]_{\text{g}}$, stirring rate, stirrer position, mixing time, container shape, interface area, and solution volume. Furthermore, the electrode response is relatively fast, but not instantaneous. (The 90% step response time of the electrode in a gas stream is ≤ 4 s.)

Since $K_{\text{eq}} = [\text{O}_2]_{\text{aq},\infty}/[\text{O}_2]_{\text{g}} = k_m/k_{-m}$, where $[\text{O}_2]_{\text{aq},\infty}$ is the equilibrium concentration of dissolved oxygen, then

$$k_m[\text{O}_2]_{\text{g}} = k_{-m}[\text{O}_2]_{\text{aq},\infty} \quad (4)$$

Substitution of eq 4 into the rate law yields

$$d[\text{O}_2]_{\text{aq}}/dt = k_m[\text{O}_2]_{\text{aq},\infty} - k_{-m}[\text{O}_2]_{\text{aq}} = k_{-m}([\text{O}_2]_{\text{aq},\infty} - [\text{O}_2]_{\text{aq}}) \quad (5)$$

Standard integration between the limits of $[\text{O}_2]_{\text{aq}} = 0$ at time = 0 and $[\text{O}_2]_{\text{aq}}$ at time = t , followed by exponentiation and rearrangement, gives

$$[\text{O}_2]_{\text{aq}} = [\text{O}_2]_{\text{aq},\infty}(1 - e^{-k_{-m}t}) \quad (6)$$

where $[\text{O}_2]_{\text{aq},\infty} = 17.9 \mu\text{M}$ under the standard conditions used in these experiments.²⁴ Rearrangement and linearization of eq 6 by taking logs of each side will yield $-k_{-m}$ as the slope of the line of the plot of $\ln([\text{O}_2]_{\text{aq},\infty} - [\text{O}_2]_{\text{aq}})$ vs time (see Figure 1). Earlier, we mistakenly claimed that the slope was the forward mass transport constant, $-k_m$.²⁴ However, as demonstrated here, it is the reverse constant, $-k_{-m}$, which is obtained directly from the slope, and k_m is subsequently computed from k_{-m} and the equilibrium constant. This counterintuitive outcome stems from the initial conditions (an open system, since $[\text{O}_2]_{\text{g}} = \text{constant}$) and the equilibrium model of the system.^{32,33}

Differentiation of eq 6 results in

$$d[\text{O}_2]_{\text{aq}}/dt = k_{-m}[\text{O}_2]_{\text{aq},\infty}e^{-k_{-m}t} \quad (7)$$

Substitution from eq 4 allows eq 7 to be rewritten as

$$d[\text{O}_2]_{\text{aq}}/dt = k_m[\text{O}_2]_{\text{g}}e^{-k_{-m}t} \quad (8)$$

which shows that the initial rate of increase in dissolved oxygen

(as $t \rightarrow 0$) is proportional to k_m and $[\text{O}_2]_{\text{g}}$, which is more in agreement with intuitive expectations. However, eq 8 also shows that as equilibrium is approached, the rate of oxygen influx is attenuated by the exponential factor which is dependent on k_{-m} , the apparent mass transport constant of oxygen out of solution.

The oscillator initiation procedure involves purging the solution with nitrogen; the 1.50% oxygen stream is then turned on and nearly immediately $[\text{O}_2]_{\text{g}} = 613 \mu\text{M}$ under standard conditions. Dissolved oxygen is monitored from 0 to 25 min (see Figure 1), and the resultant first-order exponential growth plot is linearized using eq 6. $[\text{O}_2]_{\text{aq},\infty}$ is optimized to yield a minimum error in k_m ; typically, $k_m = 0.150 \text{ min}^{-1} \pm 0.05\%$.²⁴ The excellent linearity indicates that the oxygen mass transport and dissolution process is first order under stirred conditions. Since $K_{\text{eq}} = k_m/k_{-m} = 0.0292$ (at 25 °C, 0.1 M ionic strength; computable from oxygen solubility tables),^{24,34} then typically, $k_m = 0.0044 \text{ min}^{-1}$. The resultant rate expression for the mass transport of oxygen at 25 °C is

$$d[\text{O}_2]_{\text{aq}}/dt = k_m[\text{O}_2]_{\text{g}} - k_{-m}[\text{O}_2]_{\text{aq}} = k_{-m}(K_{\text{eq}}[\text{O}_2]_{\text{g}} - [\text{O}_2]_{\text{aq}}) \quad (9)$$

where $k_m = 0.150 \text{ min}^{-1}$, $K_{\text{eq}} = 0.0292$, $[\text{O}_2]_{\text{g}} = 613 \mu\text{M}$, and $[\text{O}_2]_{\text{aq}}$ is in μM . It is important to distinguish the influx of oxygen across the gas/liquid interface from the level of dissolved oxygen in solution. When the dissolved oxygen concentration is low, the gas/liquid oxygen gradient is high and the rate of oxygen influx across the interface is high (see eq 3). Conversely, when the dissolved oxygen level is high, influx is low.

Numerical integration³⁵ of the rate law for oxygen dissolution using the typical values for k_m and k_{-m} stated above results, of course, in an exponential growth curve virtually identical to experimental data. Incorrect assignment of the measured rate constant (i.e., $k_m = 0.150 \text{ min}^{-1}$; $k_m = 5.17 \text{ min}^{-1}$) significantly changes the curve. The result is still exponential and has the correct maximum, but analysis of eq 8 shows that such a plot has an initial slope too high by a factor of $0.150/0.0044 \approx 34$, and a half-life shortened to 0.13 min, compared to the correct half-life of 4.6 min. This highlights the danger of using scaled rate constants which can yield good qualitative agreement with experimental data, but very poor quantitative agreement.

In many past studies,³⁶⁻⁴¹ the mass transport constant, k_m , was often designated k_t , and described as a diffusion constant in the expression

$$\text{oxygen diffusion rate} = k_t([\text{O}_2]_{\text{aq},\infty} - [\text{O}_2]_{\text{aq}}) \quad (10)$$

This is similar in form to eq 5 but does not actually represent a diffusion rate. In the type of stirred system used in studying peroxidase-NADH oscillations, the oxygen dissolution process is mass-transport limited and not diffusion limited, as evidenced by the fact that an increase in stirring rate causes an increase in k_m .²⁴ Were the process of oxygen dissolution presented in Figure 1 diffusion limited, k_m would be unaffected by an increased stirring rate and the equilibration time would be much faster. The mass-transport limitation is what makes the equilibration process rather slow.

In modeling efforts over the years, the connection between the experimentally measurable constant, k_m , and the conceptually identical k_t used in several models does not seem to have been made. Though k_t has been measured in some studies, the measured value is seldom used in a subsequent model.⁴¹⁻⁴³ Unreasonable values have been used in models for the oxygen mass transport constant, such as $k_m = 6 \text{ min}^{-1}$,³⁹ and $k_m = 60 \text{ min}^{-1}$.⁴³ In other instances, k_m was set equal to 0.1175,^{36,44-47}

0.1,^{37,40,42,47–48} or 5×10^{-5} ⁴⁹ and then used in a model with dimensionless variables. In one case, the experimentally measured value of $k_m = 0.240 \text{ min}^{-1}$ was correctly used in the model.⁵⁰ (This same paper, however, uses an HRP concentration of $60 \mu\text{M}$ in their model, compared to $0.7 \mu\text{M}$ HRP used in their experiments.) In addition to inconsistencies regarding k_m , the relationship between the forward and reverse rate constants provided by the calculated equilibrium constant, $K_{\text{eq}} = k_m/k_{-m} = 0.0292$, has been ignored. In some models, K_{eq} was used indirectly, and set equal to 1^{36,42,48} or 8.⁴⁶ In several instances, even though K_{eq} was apparently used in a particular model, its value cannot be calculated from the specified information.^{41,44–45,47} Relatively small differences in temperature and ionic strength used in various experiments cannot account for these wide discrepancies. For instance, when $K_{\text{eq}} = 8$, it is larger than the actual K_{eq} by a factor of 275. This suggests that either the true value of K_{eq} was entirely unrecognized, or K_{eq} (or the variable equivalent to k_m) was varied as a model parameter to yield desirable results. Aside from misunderstandings regarding oxygen mass transport, many oscillatory models do not even consider it.^{19,51–52}

A comprehensive model must include the correct expression for the mass transport rate of oxygen as shown in eq 9, where k_m is defined in reaction 2 and experimentally measured as briefly described above (and in detail elsewhere²⁴). Since oxygen is an important, if not master, variable in peroxidase–NADH oscillations, its proper inclusion in an experimentally based model is critical.^{23,53}

Since k_m is an apparent mass transport constant, it is a function of temperature. Any experiment which examines the effect of temperature on oscillations would need to compensate for the resultant change in k_m by altering some other experimental parameter which affects k_m (see Table 1). For instance, when the temperature is increased from 25 to 35 °C, $[\text{O}_2]_{\text{aq},\infty}$ decreases 15.7% to 15.1 μM , and K_{eq} decreases to 0.0254 (computable from ref 33). Any observed effect due to a change in temperature would be a convolution of the changes in temperature, k_m , and oxygen solubility, and not just temperature alone, as has been claimed.^{52,54}

Mass-Transport Constant, Induction Time, and Oscillatory Periods. The induction time is defined here as the time from the initial point of NADH influx to the first minimum in dissolved oxygen. The induction time and the period of the first oxygen oscillation were measured for 18 oscillatory runs (9 illuminated continuously by the deuterium lamp and 9 in darkness). The k_m value was determined for each individual experiment, but irreproducibility across the series caused k_m values to range from 0.141 to 0.208 min^{-1} . Except for this uncontrolled variation in measured k_m , the runs were performed under standard conditions (Table 1). The variation in k_m (mean = $0.165 \pm 12.0\%$ overall) is thought to originate from an inability in the present system to position the stirring device in the cuvette with high spatial reproducibility.²⁴ Figures and additional details appear in the supplemental material.

Because of the irreproducibility in achieving a particular oscillatory period, any study of the peroxidase–NADH oscillator which investigates the effect of a variable on oscillatory period must first examine the reproducibility in the period among individual experiments. In one case, for example, a 50% increase in period was attributed to the isotope effect between the use of NADH and its deuterated form, NADD, but period reproducibility was undocumented.⁵⁵ Without investigation of the precision of the particular apparatus used, any conclusion about how an experimental variable affects oscillatory period will remain uncertain.

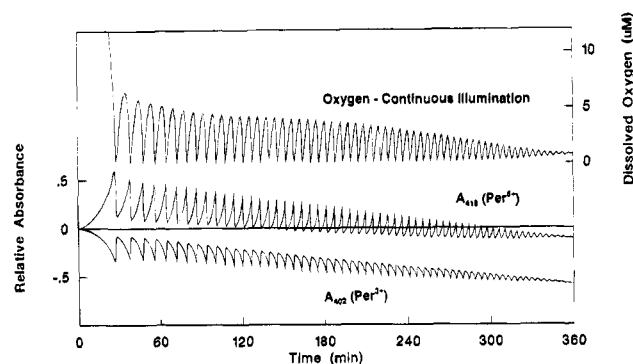


Figure 2. Standard oscillatory run under continuous illumination. Shown here are dissolved oxygen, $A_{402}(\text{Per}^{3+})$, and $A_{418}(\text{Per}^{6+})$ for the standard conditions listed on Table 1. The oxygen trace in this run also appears as the middle trace in Figure 3. This data set is excerpted from Figure 7 in ref 24.

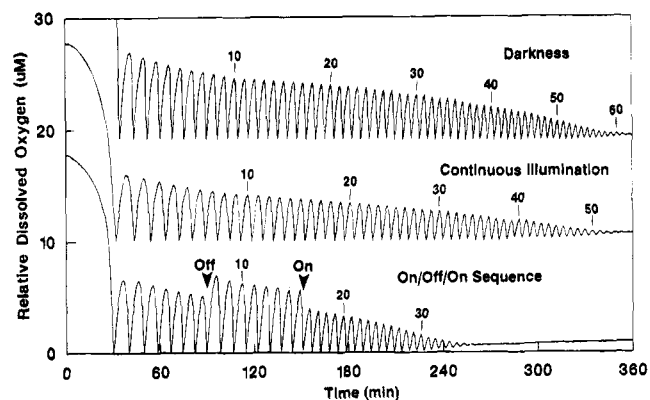


Figure 3. Illumination effects on the peroxidase–NADH oscillator. The top trace was performed under the standard conditions described in Table 1, without illumination. The middle run was made under identical conditions except with continuous illumination from the deuterium lamp in the spectrophotometer. The top two data sets are offset for clarity of presentation. The bottom run shows the effect of an on/off/on sequence of illumination under the same conditions. The lamp was off from 89.50 to 150.83 min. Peaks are numbered for comparison.

Oscillatory Damping. Figure 2 shows a standard, illuminated run including data for oxygen, $A_{402}(\text{Per}^{3+})$, and $A_{418}(\text{Per}^{6+})$. The amplitudes of all oscillations decrease over time, and the oxygen level eventually settles to a low steady state. The absorbance at the two characteristic enzyme wavelengths decreases substantially over the course of 6 h of oscillations, indicating significant alteration (presumably denaturation) of the enzyme. The decreases in the A_{402} and A_{418} maxima and minima are nearly linear, which signifies a zero-order process of enzyme depletion. The reason for enzyme depletion is presently unknown, but it could be due to attack by free radicals or H_2O_2 .⁵⁶ Additional discussion of oscillatory damping appears in the supplementary material.

Effect of Light on Oscillations. Figure 3 shows the overall effect of continuous illumination from the deuterium lamp on oxygen oscillations. The upper trace was taken in total darkness and shows damped oscillations for some 6 h. In this standard run, each successive oxygen amplitude, period, rising slope, and trailing slope is smaller than the one before. The second trace was obtained under continuous (unpulsed) illumination, but otherwise identical conditions, and demonstrates that the full spectrum of light emitted by the lamp that penetrates the sample cuvette decreases the amplitude of oxygen oscillations by about 22%. The total lifetime of the oscillator is largely unchanged, but the periods are slightly increased. In the lower trace of Figure 3, the beam path was initially unobstructed, then totally

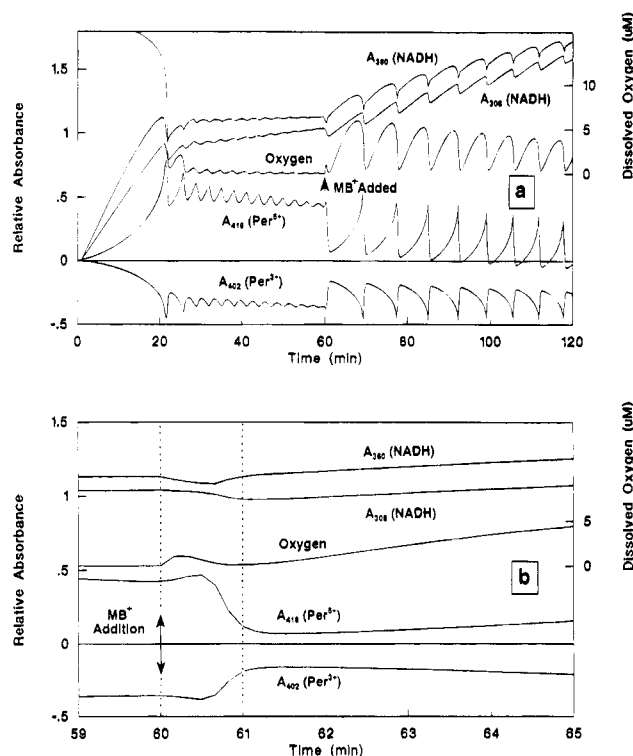


Figure 4. Addition of methylene blue. Simultaneous oxygen and absorbance data. (a) An oscillatory run was initiated under standard conditions with continuous illumination, but with the omission of methylene blue; $k_m = 0.145 \text{ min}^{-1}$. At $t = 60 \text{ min}$, MB^+ was added to bring its concentration to the standard $0.2 \mu\text{M}$. The oxygen spike from the MB^+ aliquot can be seen easily in the oxygen trace at 60 min. (b) Same data plotted on an expanded time scale.

blocked and unblocked, as shown. The attenuation effect of light on the oscillations is clearly demonstrated by a 36% increase in oxygen amplitude upon blockage of the light source. This raises the possibility that a spectroscopic experiment that involves periodic measurements which result in pulsed light exposure could excite or entrain the oscillator into some new type of behavior.⁵⁷ This is worthy of additional investigation, but continuous illumination has been used in all spectroscopic experiments in the current and most recent study.²⁴ Note in Figure 3 that the single perturbation of blocking the beam for eight periods caused oscillations to cease significantly earlier than in the other two cases. Use of cutoff filters revealed that the illumination effect is due to light of wavelength of $\leq 248 \text{ nm}$. Additional details, figures, and possible explanations appear in the supplemental material.

It should be noted that the reduced β -NADH used here forms a complex mixture of as many as six major products under mildly acidic conditions,⁵⁸ including its α anomer.⁵⁹ Since the half-life of apparent NADH degradation under illuminated conditions is about 2 h 20 min at pH 5.10,²⁴ it is expected that during an oscillatory run, a substantial portion of β -NADH is transformed to other compounds in addition to its simple oxidation product, β -NAD⁺. The effect of the presence of this complex family of β -NADH degradation compounds is unknown and entirely uninvestigated.

Omission and Then Addition of MB^+ . The oscillator was initiated in the conventional manner,²⁴ under the conditions of Table 1, but without the standard $0.2 \mu\text{M}$ MB^+ . Figure 4 shows spectroscopic and oxygen data first without MB^+ and then followed by addition of MB^+ at 60 min. The spectrophotometer was blanked (at all wavelengths) just prior to the beginning of NADH influx. Relative absorbance is therefore measured with

respect to the initial conditions which exist just before NADH influx is begun at $t = 0$. Recall that the NADH influx is relatively fast until the second oxygen minimum and then it is decreased to a maintenance level when the second oxygen minimum is observed and not changed again (Table 1).²⁴ In the initial 60 min of Figure 4a, some 13 relatively highly damped, small-amplitude oscillations were seen.

At 60 min, MB^+ was injected into the mixture to achieve $0.2 \mu\text{M}$ MB^+ ($45 \mu\text{L}$ of $22.2 \mu\text{M}$ MB^+). The MB^+ aliquot is dispersed quickly; previous work showed that for this system stirred at 1300 rotations/min (rpm), the mixing time is $\leq 0.6 \text{ s}$.²⁴ A small spike from the oxygen in the aliquot serves as a marker on the oxygen trace in Figure 4a. The oxygen spike at 60 min in Figure 4a appears as a hump on the expanded scale of Figure 4b. Oxygen returns to its pre-spike value before it begins to increase to begin the next oscillation. Nearly immediately after the addition of the MB^+ , NADH (as monitored at A_{308}) drops slightly, but sharply, apparently due to the small oxygen spike in the MB^+ aliquot. The absorbance of NADH at 308 nm then gradually increases. For comparison, note that A_{360} reaches a minimum after the MB^+ addition and then rises gradually, but A_{308} reaches a minimum perhaps 20 s later, before increasing. Clearly, A_{308} and A_{360} do not monitor identical species. A_{308} has been claimed to be the best wavelength for NADH (most spectrally pure) in the presence of HRP species,¹⁹ so A_{360} is probably a sum of NADH and other species, perhaps the native enzyme. In the past,²⁴ A_{360} was used to monitor NADH because it is less sensitive than 340 nm, the wavelength commonly used to monitor NADH absorbance.⁵⁹

After the MB^+ addition, the absorbance of native Per^{3+} (followed at A_{402}) first slightly decreases, then sharply increases. Per^{6+} (A_{418}) does essentially the opposite, first slightly increasing before it plummets downward. The slight changes in A_{402} and A_{418} in the first 30 s after MB^+ addition are probably due to the oxygen spike in the MB^+ aliquot. It would be expected that an oxygen spike would consume NADH and result in the conversion of native enzyme to Per^{6+} . This is precisely the series of events seen in Figure 4b in the 30 s immediately following MB^+ addition. After a lag time of about 30 s, the absorbance increases for Per^{3+} and decreases for Per^{6+} . Only after a lag time of 60 s is an increase seen in the level of oxygen along with a corresponding increase in the apparent NADH concentration, indicating a reduction in NADH consumption. Note that Per^{6+} and Per^{3+} have reached their respective minima and maxima about 1 min after MB^+ addition ($t = 61 \text{ min}$), but oxygen is just starting to rise, accompanied by a more gradual increase in Per^{6+} and a decrease in Per^{3+} . The most rapid changes in the enzyme absorbance occurred in the interval of 30–60 s after the MB^+ addition, as easily seen in Figure 4b. *The direct or indirect effect of MB^+ addition is to first enhance the conversion of Per^{6+} to Per^{3+} and then inhibit the consumption of oxygen and NADH, which results in the initiation of relatively large and prolonged oscillations.*

After MB^+ addition, oscillations continued for approximately 4 h. Oscillations after the initial omission, then later addition of MB^+ (as in Figure 4a) are indistinguishable from oscillations where MB^+ is present initially.²⁴ In Figure 4a, the slopes of some of the large, sharp changes in A_{402} (increases) and A_{418} (decreases) were examined. For each portion of the data set, the slopes of the initial two oscillations without MB^+ , and the slopes of the first two oscillations with MB^+ present were not significantly different. It should also be noted that the addition of MB^+ caused the periods to increase by about a factor of 2.5. This, too, suggests an overall inhibition of oxygen and NADH consumption after MB^+ addition.

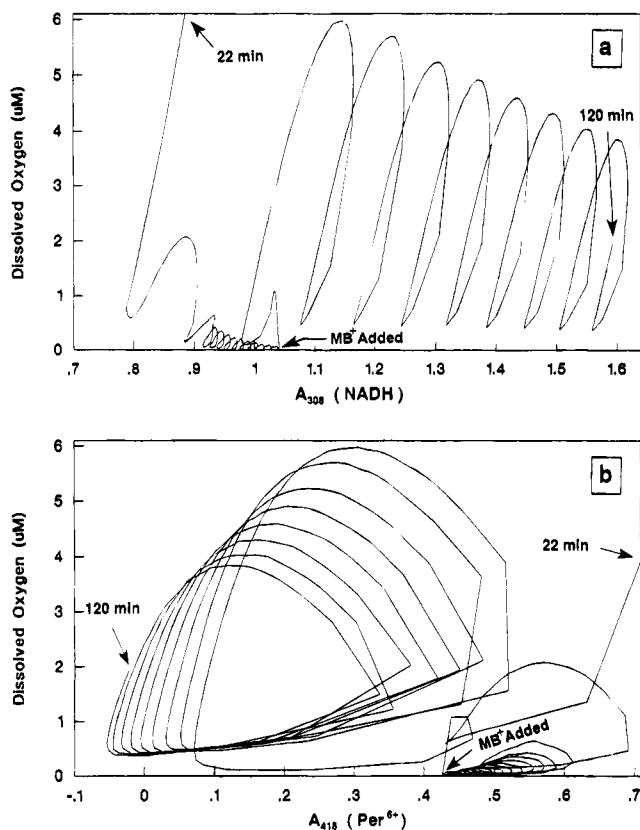


Figure 5. (a) Phase portrait for oxygen and NADH (A_{308}). (b) Phase portrait for oxygen and Per^{6+} (A_{418}). Data from Figure 4 in the region 22–120 min including the addition of MB^+ , as indicated.

The experiment and results depicted in Figure 4 are generally similar to experiments which substituted NADPH for the NADH used here and also utilized glucose-6-phosphate dehydrogenase.^{52,60} In addition, one of the studies used lactoperoxidase in place of HRP.⁶⁰ Figure 4 presents the first such data for the HRP–NADH system.

Three observations suggest that MB^+ functions as a catalyst. First, MB^+ is present in a relatively small concentration compared to other species present initially, but oscillations persist for several hours, implying that MB^+ is recycled. Second, adding an additional $0.2 \mu\text{M}$ MB^+ after oscillations have completely damped does not revive oscillatory behavior (data not shown), so apparently oscillations cease for a reason other than MB^+ depletion. Third, a small amount of MB^+ has a dramatic effect on dynamics, as is often the case with a catalyst. Larger amounts of MB^+ seem to have the same effect as $0.2 \mu\text{M}$. Only recently has MB^+ been included in a model of the peroxidase–NADH oscillator.²³ Since a catalyst increases the rate of a reaction, it must appear in the corresponding rate expression, and can often appear in a higher power than it does in the stoichiometric reaction.⁶¹ The fact that a species is a catalyst does not warrant its omission from rate equations or models (as has been claimed⁴¹), but indeed, makes its inclusion even more important.

Phase Portraits and MB^+ Addition. The phase relations among oxygen, NADH (A_{308}), and Per^{6+} (A_{418}) are explored in Figure 5. In Figure 5a, addition of MB^+ causes the general appearance of the peaks to change from small peaks with loops to much larger peaks that still cross back on themselves. According to the phase portrait in Figure 5a, the interaction between oxygen and NADH does not fundamentally change upon MB^+ addition.

In contrast, it was shown that MB^+ catalyzes the aerobic oxidation of NADH by oxygen at pH 9, with a second-order

rate constant of $k = 5.21 \text{ M}^{-1} \text{ s}^{-1}$.¹³ MB^+ also enhances NADH degradation at lower pH values with a rate constant of $k = 18 \text{ M}^{-1} \text{ s}^{-1}$ at pH 8.⁶² In both cases, the initial dissolved oxygen concentration was $249 \mu\text{M}$ (from saturation with air). The MB^+ -catalyzed oxidation of NADH yields H_2O_2 from the reduction of oxygen by the reduced form of MB^+ . This reaction could be the initial source of H_2O_2 in the oscillator. However, our studies at pH 5.10, 0.1 M NaAc, under conditions of $17.9 \mu\text{M}$ oxygen (corresponding to saturation with 1.50% O_2) using the standard $0.2 \mu\text{M}$ MB^+ show only a small enhancement of the pseudo-first-order degradation rate constant for NADH as monitored at 340 nm. We earlier showed that under continuous illumination (100% illumination duty cycle from the spectrophotometer lamp), and at pH 5.10, 25 °C, in the absence of MB^+ and oxygen, the pseudo-first-order rate constant for the degradation of 0.1 mM NADH was $k'_{\text{D},100} = 8.30 \times 10^{-5} \text{ s}^{-1} \pm 4.9\%$.²⁴ An otherwise identical triplicate determination in the absence of MB^+ , but in the presence of $17.9 \mu\text{M}$ O_2 (under humidified 1.50% O_2) gave $k'_{\text{D},100} = 8.58 \times 10^{-5} \text{ s}^{-1} \pm 4.1\%$. These two values do not differ significantly at the 90% confidence level using the computed *t*-test statistic for comparison of means.⁶³ In addition, an otherwise identical triplicate determination in the presence of $0.2 \mu\text{M}$ MB^+ and $17.9 \mu\text{M}$ O_2 gave $k'_{\text{D},100} = 9.11 \times 10^{-5} \text{ s}^{-1} \pm 4.7\%$. These last two rate constants do not differ significantly at the 90% confidence level. However, the rate constant for NADH degradation in the absence of MB^+ and O_2 , and the same constant in the presence of $0.2 \mu\text{M}$ MB^+ and $17.9 \mu\text{M}$ O_2 do differ significantly at the 90% (but not the 95%) confidence level. So, under otherwise identical conditions, upon addition of MB^+ and O_2 , the NADH degradation rate constant increased 9.8%, barely a statistically significant increase. As evidenced by the phase portrait in Figure 5a, the slight increase in NADH degradation caused by the addition of $0.2 \mu\text{M}$ MB^+ at pH 5.10 has little outward effect on the relative reactivity between NADH and oxygen. Nonetheless, such a seemingly small effect could lead to a large change in the overall behavior of a nonlinear system. The possibility remains that addition of MB^+ significantly perturbs the oscillator via a slight increase in the rate of NADH degradation and subsequent H_2O_2 production.

In Figure 5b, the relation of oxygen to Per^{6+} (A_{418}) is shown before and after MB^+ addition. Before MB^+ is added, the absorbance of Per^{6+} changes substantially during an oscillation, while the oxygen level changes a relatively small amount (0–0.5 μM). But, after MB^+ addition, the phase portrait takes on a different shape, and the ratio of the oxygen amplitude to the A_{418} amplitude has substantially increased. To quantitatively demonstrate the relative changes in O_2 and A_{418} before and after MB^+ addition, it is useful to compute the ratio of $\Delta\text{O}_2/\Delta A_{418}$ for a corresponding pair of oscillations. Let the ratio for the rise (R_r) and fall (R_f) be referenced to the oxygen oscillation. As an example, for the third oxygen oscillation after $t = 0$ (before MB^+ addition), and its corresponding A_{418} oscillation, $R_r = 2.77$ and $R_f = 3.46$. In contrast, for the third oxygen and A_{418} oscillations after MB^+ addition, $R_r = 10.5$ and $R_f = 10.5$. So, R_r increases by a factor of 3.8 upon MB^+ addition, and R_f increases by a factor of 3.0. So, ΔO_2 increases with respect to the corresponding ΔA_{418} upon addition of MB^+ .

The phase portrait in Figure 5b and the analysis of ratios suggest that MB^+ alters, either directly or indirectly, the reaction between oxygen and the enzyme in a way that inhibits O_2 consumption. The MB^+ addition data in Figure 4 clearly demonstrate that oxygen consumption is inhibited by addition of MB^+ . The overall result of the presence of MB^+ is to decrease oxygen consumption, thereby allowing an increase in

oxygen amplitudes. Since addition of MB^+ is seen to cause the inhibition of oxygen and NADH consumption, MB^+ could function as an inhibitor of a reaction which consumes oxygen or NADH. This suggests that MB^+ could act as a peroxidase inhibitor in the oxidation of NADH by O_2 . The other possibility, as discussed before, is that MB^+ could operate to increase the extent of some existing reactions, which supports the earlier suggestion that MB^+ serves as a catalyst. Exactly what MB^+ might inhibit or catalyze and why oxygen consumption decreases when MB^+ is added remain open to investigation. Other phase portraits only indicate an increase in oscillatory amplitude among the interactions of $\text{Per}^{3+}/\text{Per}^{6+}$, $\text{NADH}/\text{Per}^{6+}$, and NADH/O_2 upon addition of $0.2 \mu\text{M}$ MB^+ (see supplemental material). Other reactions of MB^+ are discussed in the supplemental material.

Conclusions

In the peroxidase–NADH oscillator system described here, it was derived that the macroscopic appearance of the process of oxygen dissolution from the gas phase is dependent on k_m , the mass-transport constant of oxygen out of solution. Oxygen dissolution is mass-transport limited and not controlled by diffusion. The rate expression for the mass transport of oxygen under the conditions of these experiments appears in eq 9. Neither the induction time of the oscillator, nor the period of the first oscillation is proportional to k_m (see supplemental material), which is not a well-controlled variable under usual conditions.

The amplitude of oxygen oscillations is decreased about 22% under continuous illumination by the deuterium source in the diode array spectrophotometer used here for absorption measurements. This attenuation effect of light is dependent on wavelengths $\leq 248 \text{ nm}$. The effect of light from the deuterium lamp which increases the autodegradation rate constant of NADH is also due to wavelengths below 248 nm (see supplemental material). The involvement of free radicals in this effect is suggested.

Initial omission of methylene blue in the oscillator allows several damped oscillations of small amplitude. Subsequent addition of MB^+ results in oscillations of much larger amplitude, revealing that MB^+ is the key to establishment of prolonged, relatively large oscillations. MB^+ is seen to either directly or indirectly enhance the conversion of Per^{6+} to Per^{3+} and then inhibit oxygen consumption. Phase portraits suggest that MB^+ changes the chemical interaction between oxygen and the enzyme. Addition of MB^+ causes the change in oxygen concentration in a given oscillation to increase by about a factor of 4 compared to the corresponding change in enzyme concentration. MB^+ could operate as a catalyst to increase the amplitude of oscillations, or as an inhibitor of peroxidase to decrease the consumption of O_2 in the enzyme-catalyzed oxidation of NADH. MB^+ could also have a dual role as catalyst of one reaction and inhibitor of another.

Many questions remain about the chemical basis of the peroxidase–NADH oscillator, but the systematic experimental strategy taken here has uncovered fresh insights about its fundamental aspects.²³ It is clear that MB^+ plays a major role in the commonly observed, relatively large oscillations of the peroxidase–NADH system. This work should allow easier corroborative efforts and lead to an improved model based on stronger correlation between theoretical predictions and experimental conditions and results. Pursuit of these goals should lead to an improved ability to investigate, understand, and eventually control or modify the role of enzymes in the regulation of oscillatory reactions and cyclic processes in biological systems.

Acknowledgment. The helpful comments of Ewa Kirkor toward the preparation of this paper and the work of Erik Williksen toward the compilation of our kinetics data base are greatly appreciated. This research has been supported in part by NSF Grant CHE-93-07549.

Supplementary Material Available: Additional material is available on topics indicated in the text (12 pages). To order, see any current masthead page.

References and Notes

- (1) Chance, B.; Pye, K.; Higgins, J. *Inst. Elect. Electron. Eng. Spectrum* **1967**, *4*, 79.
- (2) Baldwin, J. E.; Morris, G. M.; Richards, W. G. *Proc. R. Soc. London, B* **1991**, *245*, 43.
- (3) Halliwell, B. *Nature* **1991**, *354*, 191.
- (4) Murray, J. D. *Mathematical Biology: Biomathematics*; Springer-Verlag: New York, 1989; Vol. 19, pp 140–178.
- (5) Helmreich, E. J. M. In *The Molecular Basis of Circadian Rhythms*; Hastings, J. W., Schweiger, H., Eds.; Abakon Verlagsgesellschaft: Berlin, 1975; pp 157–174.
- (6) Olsen, L. R.; Frisch, L. H.; Schaffer, W. M. In *A Chaotic Hierarchy*; Baier, G., Ed.; World Scientific: London, 1991; pp 299–315.
- (7) Yamazaki, I.; Yokota, K.; Nakajima, R. *Biochem. Biophys. Res. Comm.* **1965**, *21*, 582.
- (8) Epstein, I. R. *Chem. Eng. News* **1987**, *65*, 24.
- (9) Noyes, R. M. *React. Kinet. Catal. Lett.* **1990**, *42*, 169.
- (10) Dunford, H. B. In: *Peroxidases in Chemistry and Biology*; Vol. 2; Everse, J., Everse, K. E., Grisham, M. B., Eds.; CRC Press: Ann Arbor, MI, 1991; pp 1–24.
- (11) Yamazaki, I.; Yokota, K. *Mol. Cell. Biochem.* **1973**, *2*, 39.
- (12) Alexandre, S.; Dunford, H. B. *Biophys. Chem.* **1991**, *40*, 189.
- (13) Sevcik, P.; Dunford, H. B. *J. Phys. Chem.* **1991**, *95*, 2411.
- (14) Degn, H. *Nature* **1968**, *217*, 1047.
- (15) Olsen, L. F.; Degn, H. *Nature* **1977**, *267*, 177.
- (16) Olsen, L. F. *Z. Naturforsch.* **1979**, *34A*, 1544.
- (17) Olsen, L. F. *Phys. Lett.* **1983**, *94A*, 454.
- (18) Geest, T.; Steinmetz, C. G.; Larter, R.; Olsen, L. F. *J. Phys. Chem.* **1992**, *96*, 5678.
- (19) Yokota, K.; Yamazaki, I. *Biochemistry* **1977**, *16*, 1913.
- (20) Aguda, B. D.; Larter, R. *J. Am. Chem. Soc.* **1990**, *112*, 2167.
- (21) Aguda, B. D.; Larter, R. *J. Am. Chem. Soc.* **1991**, *113*, 7913.
- (22) Olson, D. L.; Scheeline, A. *Anal. Chim. Acta* **1990**, *237*, 381.
- (23) Olson, D. L.; Williksen, E. P.; Scheeline, A. *J. Am. Chem. Soc.*, in press.
- (24) Olson, D. L.; Scheeline, A. *Anal. Chim. Acta* **1993**, *283*, 703.
- (25) Harkin, J. M.; Obst, J. R. *Science* **1973**, *180*, 296.
- (26) Gross, G. G.; Janse, C.; Elstner, E. F. *Planta* **1977**, *136*, 271.
- (27) Halliwell, B. *Planta* **1978**, *140*, 81.
- (28) Lazar, J. G.; Ross, J. *Science* **1990**, *247*, 189.
- (29) Lazar, J. G.; Ross, J. *J. Chem. Phys.* **1990**, *92*, 3579.
- (30) Samples, M. S.; Hung, Y.; Ross, J. *J. Phys. Chem.* **1992**, *96*, 7338.
- (31) Hauck, T.; Schneider, F. W. *J. Phys. Chem.* **1993**, *97*, 391.
- (32) Connors, K. A. *Chemical Kinetics: The Study of Reaction Rates in Solution*; VCH: New York, 1990; Chapter 3.
- (33) Espenson, J. H. *Chemical Kinetics and Reaction Mechanisms*; McGraw-Hill: New York, 1981; Chapter 3.
- (34) Clesceri, L. S.; Greenberg, A. E.; Trussel, R. R., Eds. *Standard Methods for the Examination of Water and Wastewater*, 17th ed.; American Public Health Association: Washington, DC, 1989.
- (35) Chesick, J. P. *J. Chem. Educ.* **1988**, *65*, 599.
- (36) Degn, H.; Olsen, L. F.; Perram, J. W. *Ann. N.Y. Acad. Sci.* **1979**, *316*, 623.
- (37) Olsen, L. F. *Z. Naturforsch.* **1985**, *40A*, 1283.
- (38) Aguda, B. D.; Frische, L. H.; Olsen, L. F. *J. Am. Chem. Soc.* **1990**, *112*, 6652.
- (39) Aguda, B. D.; Larter, R. *J. Am. Chem. Soc.* **1991**, *113*, 7913.
- (40) Watanabe, N.; Inaba, H. *Photochem. Photobiol.* **1993**, *57*, 570.
- (41) Steinmetz, C. G.; Geest, T.; Larter, R. *J. Phys. Chem.* **1993**, *97*, 5649.
- (42) Olsen, L. F.; Degn, H. *Biochim. Biophys. Acta* **1978**, *523*, 321.
- (43) Aguda, B. D.; Larter, R. *J. Am. Chem. Soc.* **1990**, *112*, 2167.
- (44) Steinmetz, C. G.; Larter, R. *J. Chem. Phys.* **1991**, *94*, 1388.
- (45) Larter, R.; Steinmetz, C. G. *Philos. Trans. R. Soc. London A* **1991**, *337*, 291.
- (46) Larter, R.; Bush, C. L.; Lonis, T. R.; Aguda, B. D. *J. Chem. Phys.* **1987**, *87*, 5765.
- (47) Larter, R.; Olsen, L. F.; Steinmetz, C. G.; Geest, T. In *Chaos in Chemistry and Biochemistry*; Field, R. J., Györgyi, L., Eds.; World Scientific: London, 1993.

- (48) Olsen, L. F. In *Stochastic Phenomena and Chaotic Behavior in Complex Systems*; Schuster, P., Ed.; Springer-Verlag: Berlin, 1984.
- (49) Fed'kina, V. R.; Bronnikova, T. V.; Ataulakhanov, F. I. *Biophysics* **1992**, *37*, 781.
- (50) Geest, T.; Olsen, L. F.; Steinmetz, C. G.; Larter, R.; Schaffer, W. M. *J. Phys. Chem.* **1993**, *97*, 8431.
- (51) Yamazaki, I.; Yokota, K. In *Biological and Biochemical Oscillators*; Chance, B., Pye, E. K., Ghosh, A. K., Hess, B., Eds.; Academic Press: New York, 1973.
- (52) Yamazaki, I.; Ishikawa, T.; Nakamura, M.; Yokota, K.; Nakamura, S. In *Biological Rhythms and Their Central Mechanism*; Suda, M., Hayaishi, O., Nakagawa, H., Eds.; Elsevier: New York, 1979; pp 19–28.
- (53) Olson, D. L. Ph.D. Thesis, University of Illinois, 1994.
- (54) Fed'kina, V. R.; Bronnikova, T. V.; Ataulakhanov, F. I. *Studia Biophys.* **1981**, *82*, 159.
- (55) Rys, P.; Wang, J. *Biochem. Biophys. Res. Comm.* **1992**, *186*, 612.
- (56) Arnao, M. B.; Acosta, M.; del Rio, J. A.; Varon, R.; Garcia-Canovas, F. *Biochim. Biophys. Acta* **1990**, *1041*, 43.
- (57) Fed'kina, V. R.; Ataulakhanov, F. I.; Bronnikova, T. V. *Theoret. Exp. Chem.* **1988**, *24*, 165.
- (58) Miksic, J. R.; Brown, P. R. *Biochemistry* **1978**, *17*, 2234.
- (59) Oppenheimer, N. J. In *Pyridine Nucleotide Coenzymes*; Dolphin, D., Avramovic, O., Poulson, R., Eds.; John Wiley: New York, 1987; Vol. 2, Part A.
- (60) Nakamura, S.; Yokota, K.; Yamazaki, I. *Nature* **1969**, *222*, 794.
- (61) In ref 32, p 263.
- (62) Williams, III, D. C.; Seitz, W. R. *Anal. Chem.* **1976**, *48*, 1478.
- (63) Bhattacharyya, G. K.; Johnson, R. A. *Statistical Concepts and Methods*; Wiley: New York, 1977.

JP941262O